Anomalous Helmholtz-Capacitance on Stepped Surfaces of Silver and Gold

Guillermo Beltramo, Margret Giesen, and Harald Ibach*

Institute for Bio- und Nano-Systems (IBN), Jülich Forschungszentrum

D 52425 Jülich

Abstract

We have studied the capacitance of the solid/electrolyte interface on Ag(11*n*) and Au(11*n*) surfaces in $KClO_4$ and $HClO_4$ as function of the electrolyte concentration and the step density. We find that the inner layer capacitance (Helmholtz-capacitance) at the potential of (total) zero charge is dramatically reduced on stepped surfaces. Standard theories which describe the Helmholtz-capacitance by properties of the liquid, a hard wall boundary condition and the polarizability of the electron gas at the metal surface fail to describe this behavior. We propose that the different polarizability of water bonded to the surface need be taken into account and attribute the reduced capacitance at steps to the lower polarizability of water molecules bonded to step edges.

*corresponding author, h.ibach@fz-juelich.de

1. Introduction

The measurement of the interfacial capacitance is a standard method to characterize the solid/electrolyte interface, in particular for metals that are approximate realizations of an ideally polarizable electrode such as gold and silver. The total capacitance of an ideally polarizable electrode, as it is measured experimentally, appears to consist of two contributions in series, the concentration-dependent Gouy-Chapman capacitance of the electrolyte and the capacitance of the inner layer at the interface, also known as the *compact layer* or the *Helmholtz-layer*. By measuring the concentration dependence of the total capacitance the two contributions are easily separated, at least at the minimum of the Gouy-Chapman capacitance which is at or near potential of zero charge (*pzc*) [1, 2]. While the capacitance of the liquid part of the electrolyte is well understood and easily calculated by solving the Poisson-Boltzmann equation (Gouy-Chapman Theory [3, 4]) the nature of the Helmholtz-layer and its contribution to the capacitance has remained elusive despite substantial research efforts. The electrical behavior of the total capacitance as being one of two capacitances in series is reproduced by theoretical approaches that take the finite size of the water molecules and ions in solution into account. In the simplest approach water and ions are represented as spheres, the spheres representing water carry a dipole moment, and the solid is represented by a "hard wall" (*mean spherical approximation,* MSA). The hard wall boundary condition leads to oscillations in the probability to find water molecules at a particular distance from the surface which causes potential oscillations as function of the distance. The deviation from the smooth exponential decay of the potential as calculated with the Gouy-Chapman model gives rise to electrical properties which are equivalent to that of a Gouy-Chapman capacitance and a concentration independent Helmholtz-capacitance in series. No inner layer with special physical and dielectric properties need be invoked. For a review of the early work the reader is referred to the lucid review of Schmickler and Henderson [5]. By construction, the MSA model as well as various amendments (see e.g. [6] for a recent update) involve only the properties of the electrolyte and therefore predict a Helmholtz-capacitance that is independent of the type of solid. Schmickler and Henderson have proposed an amendment of the MSA-model by considering the electronic polarizability of the solid (metal) into account within the framework of the jellium model. In the following, the combination of MSA with the jellium model is referred to as *Schmickler-Henderson theory*. The electronic polarizability of the solid leads to an increase in the Helmholtz capacitance. Because of the jellium model the increase depends (solely) on the electron density [5]. The theory accounts reasonably well for the trend to higher Helmholtz-capacitances with increasing electron density [5]. For the two metals silver and gold studied in this paper the Schmickler-Henderson theory would call for approximately the same Helmholtz-capacitance, although application of the jellium model to these metals is questionable, in particular in the case of gold. By a self-consistent treatment of the Poisson-Boltzmann equation and the Schrödinger equation Ibach and Schmickler have recently shown that the polarizability of a jellium metal is stronger at steps than on flat surfaces [7]. One would therefore expect the Helmholtz-capacitance of stepped surfaces to be larger than the Helmholtz-capacitance of flat surfaces.

In this paper we show that expectations from hitherto existing theories fail. The Helmholtz-capacitance at *pzc* for Ag(001) is almost a factor of two larger than for Au(001), despite the nearly identical electron density. Furthermore, the Helmholtz-capacitances of stepped Ag and Au surfaces are dramatically lower than for flat surfaces by as much as 50% for the Ag(11*7*) surface. This means that around each step a stripe of 0.2-0.5nm width does not significantly contribute to the Helmholtz-capacitance. We argue that the reason for the failure of current theories rests in the neglect of the polarizability of water bonded to the metal surface.

2. Experimental

The experiments were performed on Au(11*n*) and Ag(11*n*) single crystals with $n = 5$, 7, and 11. These surfaces are vicinal to the (001)-plane, with a miscut angle θ along the atomically dense $[\bar{1}\,\bar{1}\,0]$-direction, where $\tan\theta = \sqrt{2}/n$ [8]. The ideal surface cut along the (11*n*) plane consists of equally spaced, monatomic high and parallel steps separated by (001)-oriented terraces. The mean distance between steps in the (11*n*) plane is

$$L = \frac{a_\perp}{2}(2+n^2)^{1/2}, \qquad (1)$$

with $a_\perp$ the distance between densely packed atomic rows along $[\bar{1}\,\bar{1}\,0]$ (for Au(001) $a_\perp = 0.2884$ nm and for Ag(001) $a_\perp = 0.2889$ nm). For the Au samples, we used bead-type single crystals prepared according to a method developed by Voigtländer et al. [9]. The Ag samples were cut by spark erosion from a single crystal rod. The electrodes were oriented by diffractometry and polished to the desired orientation to within 0.1°, the limit being determined by the mosaic structure of high-quality single crystals. Prior to each experiment, the Au single-crystal electrodes were flame-annealed to about 900°C and cooled down to room temperature. In the case of Ag, the single crystals were prepared by etching in a KCN-H_2O_2 solution, annealed in a H_2-flame, and cooled down to room temperature in Ar atmosphere. Afterwards, the samples were transferred to the cell under the protection of a droplet of deoxygenated water [10]. As electrolytes, we used suprapure $HClO_4$ (Merck) and $KClO_4$ (Merck) twice recrystallized, and Milli-Q water (Millipore, $18.2\,M\Omega\,cm^{-1}$). The contact between the electrode surface and the solution was made by means of the hanging meniscus method [10] under potential control. A saturated calomel electrode (SCE) served as reference electrode and a platinum foil as counter electrode. For all electrolyte concentrations used in this study we immersed the electrodes at −0.3V vs. SCE (Au) and −0.9V vs. SCE (Ag). Cyclic voltammetry and capacitance curves were recorded using a Zahner IM5 impedance potentiostat.

Au(100) surfaces are reconstructed when immersed into the electrolyte at electrode potentials below *pzc* (at about 0V vs. SCE for Au). The reconstruction is lifted for positive potentials (>0.6V SCE for $HClO_4$ electrolyte [11]). When the potential is swept back below the *pzc* of the unreconstructed surface (~40mV SCE) the unreconstructed surface remains metastable for a short, but sufficiently long time to investigate the capacitance of the unreconstructed surface. Our data on gold surfaces refer to such measurements.

Impedance spectra of (001) and stepped surfaces between 1Hz to 10kHz show a typical response of an RC-series equivalent circuit, only at higher frequencies it is possible to see a small deviation. We have also performed experiments where we used different frequencies (between 2 and 80 Hz) and different amplitudes (between 1 and 20 mV). In all these measurements, the capacitance curves exhibit merely minimal frequency dispersions indicating that the double layer is almost perfectly described by a RC-equivalent circuit diagram, in accordance with observations by Eberhardt et al. [12].

3. Results

We have measured the capacitance versus the electrode potential for the (001), (11*11*), (11*7*), and (115) surfaces for the concentrations 5mM, 10mM, 20mM, 30mM, 50mM, and 80mM $HClO_4$ (gold) and $KClO_4$ (silver). As example, we show the results for 50mM and 10mM in Fig. 1 and 2 for the potential range around *pzc*. The characteristic minimum of the capacitance marks the minimum in the Gouy-Chapman capacitance at zero potential. For the concentration range considered here the point of zero potential coincides with the potential of zero charge (*pzc*) within 1mV [6, 13]. We therefore address the minimum of the capacitance as *pzc* henceforth in the paper.

The *pzc* shifts towards the negative on stepped surfaces. As shown in detail in two previous publications the shift is proportional to the step density [14, 15]. The shift $\Delta\phi_{\mathrm{pzc}}$ is owed to the dipole moment of step atoms p_z [16]

$$\Delta\phi_{\mathrm{pzc}} = -\frac{p_z}{\varepsilon_0 a_{\|} L} \tag{2}$$

Here, ε_0 is the dielectric permeability and $a_{\|} = a_{\perp}$ is the atomic length unit along the steps. Step dipole moments always point outwards with their positive end [17], so that the shift in the *pzc* is always towards the negative. For steps on (001) surfaces of Au and Ag the step dipole moments are about 8×10^{-32} Cm and 5.6×10^{-32} Cm, respectively [14, 15].

With increasing step density also the capacitance at *pzc* shifts downwards. The downshift in the capacitance is the more pronounced the larger the concentration and thus the larger the total capacitance is. This and the fact that the downshift in the capacitance at *pzc* is observed also for all other electrolytes indicate that the Helmholtz-capacitance at *pzc* varies with the step density: the higher the step density, the lower the Helmholtz-capacitance.

We now use the concentration dependence of the capacitance to quantify this qualitative observation. In complete absence of specific adsorption of ions the Helmholtz capacitance C_{H} at *pzc* is obtained from a *Parsons-Zobel-plot* of the measured inverse total capacitance C_{tot}^{-1} vs. the calculated inverse Gouy-Chapman capacitance C_{GCh}^{-1} [12]. The small specific adsorption of $\mathrm{ClO_4^-}$ ions in our case causes a deviation from a straight line in the *Parsons-Zobel-plot*, preventing an accurate determination of C_{H}. We can safely exclude roughness as the cause for the deviations from linearity in our case (see discussion section). To account for the effect of specific adsorption on the electrical properties of the interface it proves useful to introduce a capacitance parallel to the diffuse layer capacitance as the derivative of the charge per area on the metal caused by specific adsorption $Q^{(\mathrm{spec})}$ with respect to the electrode potential ϕ [12],

$$C_{ad} = \frac{\partial Q^{(\mathrm{spec})}}{\partial \phi}. \tag{3}$$

The total capacitance is then

$$C_{tot} = C_{ad} + \frac{1}{\dfrac{1}{C_H} + \dfrac{1}{C_{GCh}}} = C_{ad} + \frac{C_H C_{GCh}}{C_H + C_{GCh}}. \tag{4}$$

At *pzc* the Gouy-Chapman capacitance C_{GCh} can be expressed in terms of the concentration as

$$C_{\mathrm{GCh}} = \varepsilon_0 \varepsilon \kappa \tag{5}$$

in which κ is the inverse of the Debye-length

$$\kappa = Ze\sqrt{2n_0 / \varepsilon_0 \varepsilon k_{\mathrm{B}} T} \tag{6}$$

with ε the relative dielectric permeability of water, n_0 the concentration of ions of one type, Z their charge number, k_{B} the Boltzmann-constant and T the temperature. Eqs. 4-6 may be written as

$$\frac{\varepsilon \varepsilon_0 \kappa}{C_{\mathrm{tot}} - C_{\mathrm{ad}}} = 1 + \frac{\varepsilon \varepsilon_0}{C_{\mathrm{H}}} \kappa \tag{7}$$

This form offers a systematic way to determine both C_{ad} and C_{H} by plotting the left hand side versus κ for various assumed values of C_{ad}. For the correct value of C_{ad} a fit through the data with a straight line intersects the ordinate exactly at 1. The slope yields the Helmholtz-capacitance C_{H}. Fig. 3 and 4 display these plots for gold and silver respectively. All data fit nicely to the linear plot and yield small values for C_{ad}, indicating that the analysis following eq. (7) is meaningful. Further contribution to eq. (7) quadratic in κ may arise from nonlocal contributions to the dielectric constant of the solvent [18], from a high concentration of ions at the interface, or from a change in the effective dielectric constant of the solute [13]. Such contributions have been observed, albeit for concentrations 10 times higher than used here [19]. They are insignificantly small in the concentration range studied here. The individual values for C_{ad} obtained from the fit to a straight line intersecting the ordinate exactly at 1 are listed in the figures. For gold surfaces, C_{ad} is identical for surfaces with different step densities within the limits of error. Fitting individual values of C_{ad} rather than a mean value for all step densities has no significant effect on the Helmholtz capacitances C_{H}. For silver, the values for C_{ad} are smaller than for gold in agreement with the lesser specific adsorption of $\mathrm{ClO_4^-}$ on silver [20]. The trend to smaller C_{ad} with higher step density in the case of silver indicates an even lesser adsorption of $\mathrm{ClO_4^-}$ at steps. Also listed in the figures are the resulting Helmholtz-capacitances. The results for the Helmholtz-capacitances are summarized in Table 1. For both materials, the Helmholtz-capacitance decreases significantly on stepped surfaces. For Au(11*n*) the decrease is linear in the step density within the limits of error (Fig. 5). For Ag(11*n*) surfaces the decrease either saturates or may even pass through a minimum at about 54% of the initial value (Fig. 5).

In order to check whether modeling of the specific adsorption with a finite shunting capacitance C_{ad} has a significant effect on the Helmholtz-capacitance we have calculated the

Helmholtz-capacitance from the slope of the data in plots such as Fig. 3/4 but with C_{ad} set to zero. In that case, the analysis of eq. (7) is mathematically, although not technically equivalent to the analysis using the *Parsons-Zobel-plot*. The results are shown in brackets in Table 1. The relative reduction in the Helmholtz-capacitance is nearly the same. On the (117) surface e.g., the Helmholtz-capacitance of gold is reduced by 18% instead of 22% and by 44% instead of 48% for silver. The obtained reduction of the Helmholtz-capacitance for stepped is therefore not an artifact of our analysis.

Further support for attributing the reduced capacitance at *pzc* solely to the Helmholtz-capacitance stems from the fact that a reduction in the total capacitance at *pzc* is observed also for H_2SO_4 and HF electrolytes. Fig. 6 shows the total capacitance C_{tot} at *pzc* vs. the step density on Au(11*n*) surfaces in 5mM HF, $HClO_4$, and H_2SO_4 as obtained in [14]. For all three electrolytes C_{tot} decreases slightly with increasing step density. The solid lines in Fig. 6 represent the capacitances calculated using eq. (4) and the linear decrease in the Helmholtz-capacitance as obtained in Fig. 5. To fit the total capacitance for the Au(001) surface C_{ad} is set to 0, 4 and 16.4 μFcm^{-2} for HF, $HClO_4$ and H_2SO_4, respectively. The required setting $C_{ad} = 0$ for the HF-electrolyte is consistent with the understanding that there is no specific adsorption of fluor at *pzc*. The larger C_{ad} for the H_2SO_4 electrolyte is consistent with the significant specific adsorption of SO_4^--ions on gold even at *pzc* [21]. The solid line fits the data for HF quite well, supporting the model of a reduced Helmholtz-capacitance at steps. For H_2SO_4 electrolyte, the experimentally observed capacitance falls below the calculated line. The additional reduction in the capacitance could arise from a reduced specific adsorption of sulfate at steps. To illustrate this point we have calculated the reduction in the capacitance under the assumption that the relative reduction in C_{ad} has the same dependence on the step density as the Helmholtz-capacitance (dashed line in Fig. 6). An alternative possibility is that the reduction of the Helmholtz capacitance is stronger with coadsorbed sulfate.

4. Discussion

4.1 Possible influence of roughness

Before entering the discussion we briefly pay attention to a possible influence of the roughness of stepped surfaces on their Gouy-Chapman capacitance. Rough surfaces may have a higher Gouy-Chapman capacitance because their microscopic area is larger than the macroscopic area. The ratio of both defines the roughness factor $R>1$. The roughness factor depends on the ratio of the characteristic length of the roughness to the Debye-length.

Applied to our problem of stepped surfaces with a step-step distance L, this means that the roughness factor R depends on the product κL. For dilute electrolytes, $\kappa L \ll 1$, the surface is smooth on the scale of the Debye-length, hence $R \approx 1$. For $\kappa L \gg 1$, R approaches the ratio of the microscopic to macroscopic surface area. For periodic profiles the roughness factor can be calculated using the work of Daikhin et al. [22]. From the discussion above we see that the lowest Fourier-component of the roughness is of prevailing importance. We may therefore describe the profile of a stepped surface as (Fig. 7)

$$z = (h/4)\sin(2\pi x/L) \tag{8}$$

where h is the step height. The roughness R then becomes [22]

$$R = 1 + \frac{h^2\kappa^2}{16}\left\{\left(1 + \frac{4\pi^2}{\kappa^2 L^2}\right)^{1/2} - 1\right\} \tag{9}$$

The maximum roughness factor is obtained for the highest concentration and the smallest distance L and amounts to 1.017. For the smallest concentration R is 1.0003. The effect of the correspondingly increased capacitances on the slopes of the linear fits in Fig. 3 and 4, and thus on the calculated Helmholtz-capacitances is therefore negligible. We note that this calculation also excludes the proposition that the deviation from the straight line in a *Parsons-Zobel plot* for single crystal surfaces could be attributed to roughness.

4.2 Helmholtz-capacitance of steps

The linear decrease of the Helmholtz-capacitance with the step density for gold surfaces points to a local effect of the steps, namely that the Helmholtz-capacitance is reduced in a stripe along each step ("*dead stripe*"). We calculate the width of these stripes in the following. On Au(11*n*) surfaces the Helmholtz-capacitance appears to decrease approximately linear with the inverse of the step density. The solid line in Fig. 5 is a fit to

$$C_{\mathrm{H}}(L^{-1})/C_{\mathrm{H}}(0) = 1 - l_{\mathrm{H}} L^{-1} \tag{10}$$

with $l_{\mathrm{H}} = 0.22$nm. In the limit that a stripe alongside each step does not contribute at all to the Helmholtz-capacitance l_{H} is the width of that stripe. If the Helmholtz-capacitance is merely reduced by a factor $\alpha < 1$, then l_{H} is

$$l_{\mathrm{H}} = l_{\mathrm{H}}^{(\mathrm{red})}(1-\alpha) \tag{11}$$

in which $l_{\mathrm{H}}^{(\mathrm{red})}$ is the width of the stripe with the reduced capacitance. The linear decrease of the Helmholtz-capacitance with L^{-1} saturates when the stripes with reduced capacitance begin to overlap. In terms of $l_{\mathrm{H}}^{(\mathrm{red})}$ the Helmholtz-capacitance is then described by

$$C_{\mathrm{H}}(L^{-1})/C_{\mathrm{H}}(0)=\begin{cases}\left(1-l_{\mathrm{H}}^{(\mathrm{red})}(1-\alpha)L^{-1}\right) & \text{if } C_{\mathrm{H}}>\alpha\, C_{\mathrm{H}}(0)\\ \alpha & \text{else}\end{cases} \tag{12}$$

We apply this model to describe the saturation of the reduction on silver surfaces. Fig 5 instructs us that the factor α should be then 0.54. From the initial slope one obtains $l_{\mathrm{H}}^{(\mathrm{red})}(\mathrm{Ag})\approx 1.2\mathrm{nm}$. The dashed line in Fig. 5 shows the fit of eq.(12) to the data with these numbers for α and $l_{\mathrm{H}}^{(\mathrm{red})}$. Assuming that the Helmholtz-capacitance on gold is reduced by the same factor $\alpha = 0.54$ one calculates $l_{\mathrm{H}}^{(\mathrm{red})}(\mathrm{Au})\approx 0.5\mathrm{nm}$ from eq. (11). In view of the scarce data point in Fig. 5 and their error bars details of his heuristic description are open. In any case, the width of the *dead stripe* is significantly larger on silver.

4.3 Microscopic models

According to the mean spherical approximation (MSA) the second term on the right hand side of eq. (7) and thus the existence of a concentration independent contribution to the capacitance follows from the finite size of ions and water molecules and the dipole moment associated with the water molecules in combination with the hard-wall boundary condition of the liquid at the solid surface [5]. In terms of the diameters of the ions d_{I} and the solvent molecules d_{s} (both considered as spheres) the inverse capacitance is

$$C_{\mathrm{tot}}^{-1}=\frac{1}{\varepsilon\varepsilon_0\kappa}+\frac{1}{2\varepsilon\varepsilon_0}\left\{d_{\mathrm{I}}+\frac{\varepsilon-1}{\lambda}d_{\mathrm{s}}\right\}-C_{\mathrm{el}}^{-1}. \tag{13}$$

The additional contribution C_{el}^{-1} describes the effect of the electronic polarizability following Schmickler and Henderson [5]. The parameter λ is obtained from the equation

$$\lambda^2(1+\lambda)^4=16\varepsilon. \tag{14}$$

For water with $\varepsilon = 80$ the parameter λ is $\lambda = 2.65$. The first term within the bracket of eq. (13) arises from the distance of closest approach of the ions from the hard wall $d_{\mathrm{I}}/2$, the second, significantly larger term is a consequence of the oscillating probability to find water molecules at a particular distance z from the surface. This stratification of the water molecules and their oscillating orientations cause corresponding oscillations in the potential, resulting in a steep potential gradient at the surface that is independent of the ion concentration in the electrolyte. The Helmholtz-capacitance is the macroscopic manifestation of that behavior.

The theory sketched above describes the Helmholtz-capacitance on mercury quite well, and also very crudely the overall trend with the electron density [5]. For gold and silver surfaces, the Schmickler-Henderson theory would call firstly for a nearly equal Helmholtz-capacitance for Au(001) and Ag(001) and secondly for a larger Helmholtz-capacitance for stepped surfaces because of the larger electronic polarizability at steps [7]. Obviously, the theory fails in both predictions, indicating that an important aspect is missing. We suggest that this aspect is the chemical bonding of first-later water molecules to the surface.

The bonding of water molecules to surfaces has been subject of intense, often controversial debate. Presently most authors have converged on a picture that involves an H-bonded network of water molecules ("bilayer model" [23, 24]) bonded to the metal surface via the oxygen lone pair electron. For a general review the reader is referred to the extensive review of Henderson [25] and to the recent comprehensive discussion of the theory by Meng et al. [26]. As already proposed in 1980 [23] hydrogen atoms that are not engaged in the H-bonding to neighboring molecules may either point towards or away from the surface (H-up and H-down configurations) (Fig. 8a). Both configurations coexist on Platinum [23] at low temperatures and have nearly equal energy with slightly higher adsorption energy for the H-down configuration on Pd surfaces [26]. As the binding energy amounts to 0.5eV per water molecule the equilibrium vapor pressure at 300K is about 0.01bar [2]. Under ultra-high vacuum conditions, the structures are therefore stable only at lower temperatures ($T \leq 150\text{K}$) [27, 28]. However in contact with liquid water at 1bar pressure a key element of the structure namely the bonding of the first layer water molecule to the metal on-top sites either via the oxygen lone-pair bond or a hydrogen bond should survive at 300K (with considerable fluctuations). This notion is corroborated by ab-initio molecular dynamical calculations of Izvekov and Voth [29]. The authors find that on uncharged Ag(111) surfaces water molecules are bonded to the on-top sites of silver atoms at a rather well defined distance of 0.215 nm. Neither the limited simulation time (1ps) nor the size of the unit cell allowed a build-up of periodic bilayer structures. Ab-initio molecular dynamics simulations of Sugino et al. on Pt(111) surfaces confirmed that water bonds via hydrogen bonds to Pt atoms for negatively charged surfaces [30]. Periodic structures or stable H-bonds between adsorbed water molecules were likewise not found in the limited space-time frame. The existence of bilayer structures on surfaces in contact with liquid water remains questionable therefore. The two configurations of first-layer water molecules, one bonded via the oxygen atom, the other via the hydrogen atom lead to different oxygen/surface distances. Such potential dependent bond distances have been found in the hitherto only experimental in-situ X-ray diffraction study by Toney et al. [31]. Unfortunately, the unacceptably high oxygen concentrations found in this study cast a shadow of doubt on this experiment. Nevertheless, the experimental oxygen/surface distances and their dependence on the surface charge agree nicely with theoretical calculations of the structure of water bilayers on palladium surfaces [32]. In summary, one may conclude that first layer water molecules are bonded to the metal surface atoms. The bonding is either via a hydrogen bond or, at positive potentials, via the oxygen lone-pair bond. The potential where the (presumably gradual) transition occurs depends on the electrode material. The Helmholtz-capacitance of flat surfaces should therefore reflect the electrical polarizability of water thus bound to the surface and is not describable as being merely a property of liquid water at a solid boundary as in the Schmickler-Henderson theory. The limitations of the Schmickler-Henderson theory are also manifest in the arrangement of oxygen atoms predicted by that theory. The Schmickler-Henderson theory produces a stratified arrangement of oxygen atoms [5] which, however, differs substantially in detail from experiment and total energy calculations that take the water/surface bond into account. We therefore conclude that the large difference in the Helmholtz-capacitances of Au(100) and Ag(100) are presumably due to differences in the polarizability of first-layer water molecules to these surfaces. Theoretical studies which compare Ag(100) and Au(100) are not available at present.

Concerning the properties of the first-layer water at steps there is ample experimental and theoretical evidence for significant difference to flat surfaces. In 1996, M. Morgenstern et al. showed that on Pt(111) water bonds to the upper edge of steps in "quasi one-dimensional chains" with a higher binding energy than on flat surfaces [27]. Similar observations on Au(100) were recently reported by K. Morgenstern [28]. Inspired by the early experiments, Meng et al. have investigated theoretically chain-like structures of water monomers at A-steps (displaying a (100) microfacet) on Pt(111) [26]. The most stable chain consists of a zigzag chain of H-bonded, essentially flat-lying water monomers with the second hydrogen atom of the monomer pointing alternately inwards and outwards of the step (Fig. 8b). According to Meng et al. the oxygen lone-pair bond energy is significantly larger at steps (0.45eV at steps vs. 0.29eV on terraces). Furthermore, unlike water in the bilayer configuration each water molecule and not every second one forms an oxygen lone-pair bond with the substrate. In agreement with the stronger oxygen-metal bonding the mean distance of the oxygen atoms to the surface is smaller than for bilayer oxygen atoms. The lower coordination of the water molecules at steps with respect to their H-bonds is thereby compensated, so that the total binding energy per molecule for water on terraces and at step in their respective structures is about the same.

We note from Fig. 8b that the inward-pointing H-atoms are not oriented in a direction suitable for H-bonding to water on terraces (Fig. 8a). These H-atoms can therefore not engage in H-bonding to water on terraces. Experimental result support this notion: Upon exposure to small doses, water adsorbs on Au(100) firstly at steps in the form of thin stripes (width < 1.0nm [27, 28]). Upon further exposure however, water does not continue to grow from the decorated steps. Instead, further adsorbed water nucleates on terraces [28]. This clearly shows that water at steps cannot engage in H-bonding. We therefore conclude that experimental and theoretical evidence support the proposition that water at steps is bonded in the form of the zigzag chains, not only on platinum but also on Au(100), and presumably on other surfaces. As in the case of flat surfaces it is not known whether the chain structure of water at steps is preserved when in contact with liquid water at 300 K. We can however safely conclude that the oxygen lone-pair bonding survives at 300 K since it does on terraces and the bond energy is nearly twice as large at steps.

Contrary to water on terraces, water at steps does not feature H-in and H-out configurations in relative concentrations which depend on the surface charge (electric field). Furthermore, all water molecules form rigid oxygen lone-pair bonds with the surface, contrary to water in the bilayer configuration where every second water molecule is bonded only via the highly flexible H-bond. The polarizability of water bonded to steps should therefore be significantly less than for water bonded to terrace atoms. We therefore identify the experimentally found *dead stripes* with the specific form of water at steps. The width of the chain-structure which is of the order of 0.3 nm (Fig. 8b) matches the width of the *dead stripe* on Au(100). The larger width found for Ag(100) indicate that other, broader structures may be involved on Ag(100). Presently, neither experimental nor theoretical intelligence regarding the structure of water at steps is available for that surface.

5. Conclusions

The Helmholtz-capacitance of stepped Au(11*n*) and Ag(11*n*) surfaces is significantly lower than the Helmholtz-capacitance of flat Au(001) and Ag(001) surfaces. On gold vicinal surfaces the reduction in the capacitance is roughly proportional to the step density, whereas on silver surfaces the reduction appears to saturate at higher step densities. This result is at variance with currently available theories. We ascribe the lower capacitance to the stronger bonding of water molecules to step sites, their different structure there, and the ensued lower polarizability; an effect not included in present theoretical treatments of the Helmholtz-capacitance.

Acknowledgement

We thank Karina Morgenstern, University Hannover, for a helpful exchange of ideas on the adsorption of water at steps and for making STM images available to us prior to publication. Inspiring discussions with Wolfgang Schmickler, University Ulm, are also gratefully acknowledged. Udo Linke has contributed significantly to this work by his careful and innovative preparation of the crystal surfaces. The work was partially supported by the Fond der Chemischen Industrie and the Deutsche Forschungsgemeinschaft.

References

[1] W. Schmickler, *Interfacial Electrochemistry*, Oxford University Press, Oxford 1995.
[2] H. Ibach, *Physics of Surfaces and Interfaces*, Springer, Berlin, Heidelberg, New York 2006.
[3] G. Gouy, J. Phys. (Paris) 9 (1910) 457.
[4] D. L. Chapman, Philos. Mag. 25 (1913) 475.
[5] W. Schmickler, D. Henderson, Progr. Surf. Sci. 22 (1986) 323.
[6] M. Valisko, D. Henderson, D. Boda, J. Phys. Chem. B 108 (2004) 16548.
[7] H. Ibach, W. Schmickler, Phys. Rev. Lett. 91 (2003) 016106.
[8] M. Giesen, Prog. Surf. Sci. 68 (2001) 1.
[9] B. Voigtlander, U. Linke, H. Stollwerk, J. Brona, J. Vac. Sci. Technol. A 23 (2005) 1535.
[10] A. Hamelin, J. Electroanal. Chem. 386 (1995) 1.
[11] E. Santos, W. Schmickler, Chem. Phys. Lett. 400 (2004) 26.
[12] D. Eberhardt, E. Santos, W. Schmickler, J. Electroanal. Chem. 419 (1996) 23.
[13] M. Valisko, D. Henderson, D. Boda, J. Molecular Liq. 131 (2007).
[14] G. L. Beltramo, H. Ibach, M. Giesen, Surf. Sci. 601 (2007) 1876.
[15] G. Beltramo, H. Ibach, U. Linke, M. Giesen, Electrochim. Acta 53 (2008) 6818.
[16] J. Lecoeur, J. Andro, R. Parsons, Surf. Sci. 114 (1982) 320.
[17] J. E. Müller, H. Ibach, Phys. Rev. B 74 (2006) 085408.
[18] A. A. Kornyshev, J. Ulstrup, J. Electroanal. Chem. 183 (1985) 387.
[19] L. Blum, D. Henderson, R. Parsons, J. Electroanal. Chem. 161 (1984) 389.
[20] G. Valette, J. Electroanal. Chem. 138 (1982) 37.
[21] Z. Shi, J. Lipkowski, S. Mirwald, B. Pettinger, J. Electroanal. Chem. 396 (1995) 115.
[22] L. I. Daikhin, A. A. Kornyshev, M. Urbakh, Phys. Rev. E 53 (1996) 6192.
[23] H. Ibach, S. Lehwald, Surf. Sci. 91 (1980) 187.
[24] D. L. Doering, T. E. Madey, Surf. Sci. 123 (1982) 305.
[25] M. A. Henderson, Surf. Sci. Rep. 46 (2002).
[26] S. Meng, E. G. Wang, S. Gao, Phys. Rev. B 69 (2004) 195404.
[27] M. Morgenstern, T. Michely, G. Comsa, Phys. Rev. Lett. 77 (1996) 703.
[28] K. Morgenstern, private communication.
[29] S. Izvekov, G. A. Voth, J. Chem. Phys. 115 (2001) 7196.
[30] O. Sugino, I. Hamada, M. Otani, Y. Morikawa, T. Ikeshoji, Y. Okamoto, Surf. Sci. 601 (2007) 5237.
[31] M. F. Toney, J. N. Howard, J. Richer, G. L. Borges, J. G. Gordon, O. R. Melroy, D. G. Wiesler, D. Yee, L. B. Sorensen, Surf. Sci. 335 (1995) 326.
[32] J.-S. Filhol, M.-L. Bocquet, Chem. Phys. Lett. 438 (2007) 203.

Tables

Table 1: Helmholtz-capacitances for Au(001) and Ag(001) vicinals as obtained from Fig. 1 and Fig. 2. The values in brackets are without taking the capacitance due to the small specific adsorption into account ($C_{\mathrm{ad}} = 0$).

Surface	(001)	(11*11*)	(11*7*)	(11*5*)
Step density L^{-1}/nm^{-1}	0	0.624	0.969	1.33
C_{H}(Au)/µFcm^{-2}	78.5±3	71.5±2	61.3±3	54.3±3
with $C_{\mathrm{ad}} \equiv 0$	(70.1)	(65.6)	(57.6)	(51.8)
C_{H}(Ag)/µFcm^{-2}	145±7	94.6±1	75.1±2	81.1±2
with $C_{\mathrm{ad}} \equiv 0$	(127)	(87.5)	(71.4)	(79.1)

Figure Captions

Fig. 1: Capacitance of Au(001), Au(11*11*), Au(11*7*), and Au(11*5*) for (a) 50mM $HClO_4$ and (b) 10mM $HClO_4$. The minima mark the potential of zero charge (*pzc*). Electrode potentials ϕ are with reference to the saturated calomel electrode (SCE).

Fig. 2: Capacitance of Ag(001), Ag(11*11*), Ag(11*7*), and Ag(11*5*) for (a) 50mM $KClO_4$ and (b) 10mM $KClO_4$. The minima mark the potential of zero charge (*pzc*).

Fig. 3: Plots of $\varepsilon\varepsilon_0\kappa/(C_{\mathrm{tot}} - C_{\mathrm{ad}})$ vs. κ for Au(*hkl*) following eq. (7). The slope is proportional to the inverse of the Helmholtz-capacitance C_{H} (see insert). The values of C_{ad} representing the capacitance at *pzc*, describing the change in the surface charge with applied voltage due to specific adsorbates, are fitted so that the least square fit straight lines pass through 1 at $\kappa = 0$.

Fig. 4: Plots of $\varepsilon\varepsilon_0\kappa/(C_{\mathrm{tot}} - C_{\mathrm{ad}})$ vs. κ for Ag(*hkl*) following eq. (7). The slope is proportional to the inverse of the Helmholtz-capacitance C_{H} (see insert). The values of C_{ad} representing the capacitance at *pzc*, describing the change in the surface charge with applied voltage due to specific adsorbates, are fitted so that the least square fit straight lines pass through 1 at $\kappa = 0$. C_{ad} is much smaller than for gold surfaces in agreement with the understanding of a lesser specific adsorption of ClO_4^- on silver.

Fig. 5: The decrease of the Helmholtz-capacitance with the inverse of the mean distance between the steps. For Au(11*n*) surfaces the decrease is linear within the limits of error (squares). This suggests within a stripe along each step the Helmholtz-capacitance is reduced ("*dead stripes*"). For Ag(11*n*) surfaces the Helmholtz-capacitance saturates for higher step densities or may even pass through a minimum. Saturation is explained by assuming that the *dead stripes* overlap for step densities beyond $L^{-1} > 0.8\mathrm{nm}^{-1}$.

Fig. 6: Comparison of capacitances at *pzc* on Au(11*n*) surfaces in 5mM H_2SO_4, $HClO_4$, and HF. For all three electrolytes the capacitance decreases with increasing step density. The solid lines are calculated assuming the same decrease in the Helmholtz-capacitance as for $HClO_4$ with C_{ad} chosen as 0, 4, and 16.4μFcm^{-2}. The dashed line is with the assumption that also the capacitance describing the specific adsorption C_{ad} decreases with increasing step density in the same way as the Helmholtz-capacitance (capacitances taken from [14]).

Fig. 7: Surface profile used to calculate the effect of the roughness of stepped surfaces on the Gouy-Chapman capacitance. The figure shows a [115] surface.

Fig. 8: (a) Low temperature structure of water in the first monolayer. The model was originally proposed by Ibach and Lehwald in 1980 based on spectroscopic evidence for all three forms of hydrogen [23]. Nevertheless it is now universally attributed to Doering and Madey [24]. On flat surfaces, water forms a bilayer in which every second water molecule bonded to the surface via the oxygen lone pair while the other water molecule interconnects those water molecules via hydrogen-bonding. Hydrogen atoms not engaged in H-bonding may either point upwards or downwards towards the metal; the latter case is indicated by a dashed circle. Recent theoretical studies show that ordered phases with hydrogen in the up and down configuration have nearly the same energy albeit with different distances for of the oxygen atom from the surface. At room temperature and in the presence of ambient water the bonding to the metal surface survives with a mixture of up- and down-configuration depending on the surface charge. The bilayer structure may not exist in contact with liquid water at 300 K.

(b) A zigzag chain of water molecules at the upper step edge as proposed by Meng et al. [26]. The binding energy per water molecule is about the same as for water on terraces [26, 27]. The hydrogen atoms pointing inward and outward of the step do not engage in hydrogen bonding to water molecules adsorbed on terraces [28]. Unlike the bilayer structure on terraces the chain structure does not offer the possibility for electric field-induced changes in the orientation of the molecules. The polarizability is therefore much lower causing the lower Helmholtz-capacitance at steps.

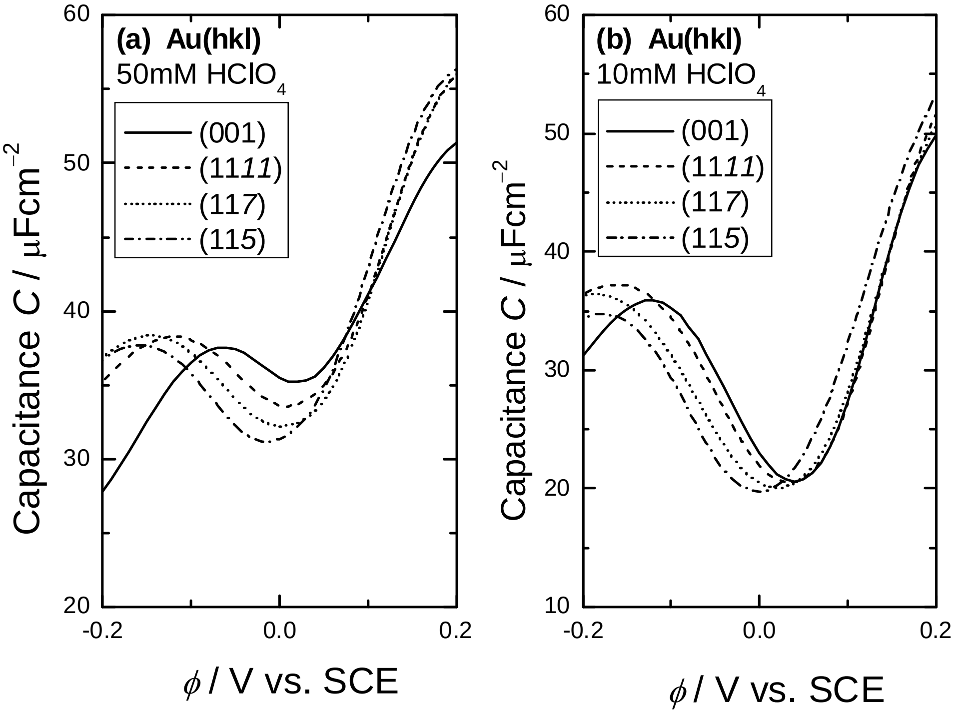
(a) Au(hkl)
50mM $HClO_4$
(001)
(11*11*)
(11*7*)
(11*5*)
Capacitance *C* / μFcm^{-2}
20
30
40
50
60
-0.2
0.0
0.2
ϕ / V vs. SCE
(b) Au(hkl)
10mM $HClO_4$
(001)
(11*11*)
(11*7*)
(11*5*)
Capacitance *C* / μFcm^{-2}
10
20
30
40
50
60
-0.2
0.0
0.2
ϕ / V vs. SCE

Fig. 1

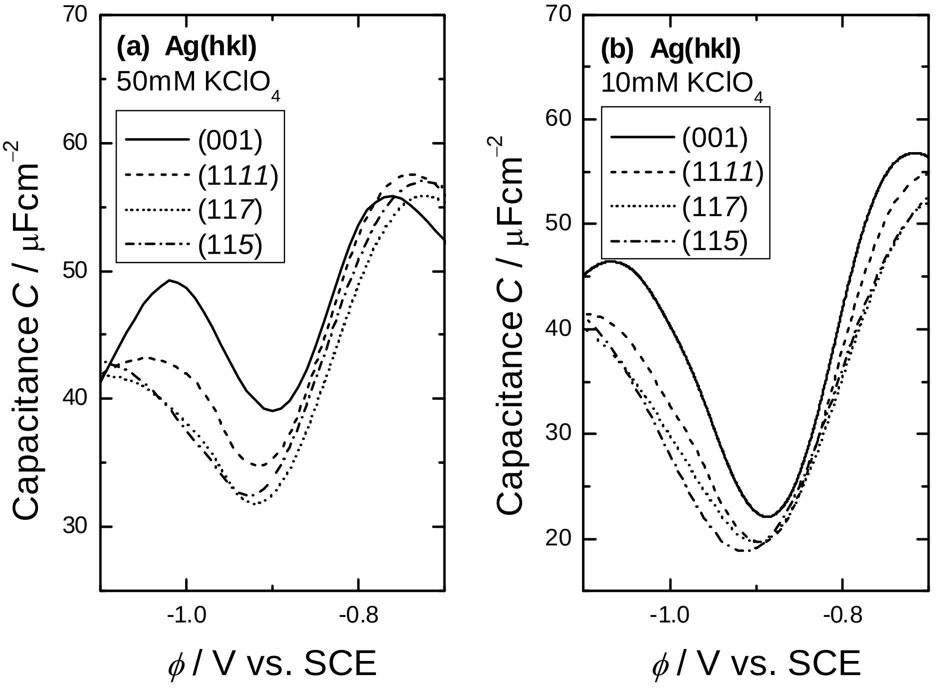
(a) Ag(hkl)
50mM $KClO_4$
(001)
(11*11*)
(11*7*)
(11*5*)
Capacitance *C* / μFcm^{-2}
30
40
50
60
70
-1.0
-0.8
ϕ / V vs. SCE
(b) Ag(hkl)
10mM $KClO_4$
(001)
(11*11*)
(11*7*)
(11*5*)
Capacitance *C* / μFcm^{-2}
20
30
40
50
60
70
-1.0
-0.8
ϕ / V vs. SCE

Fig. 2

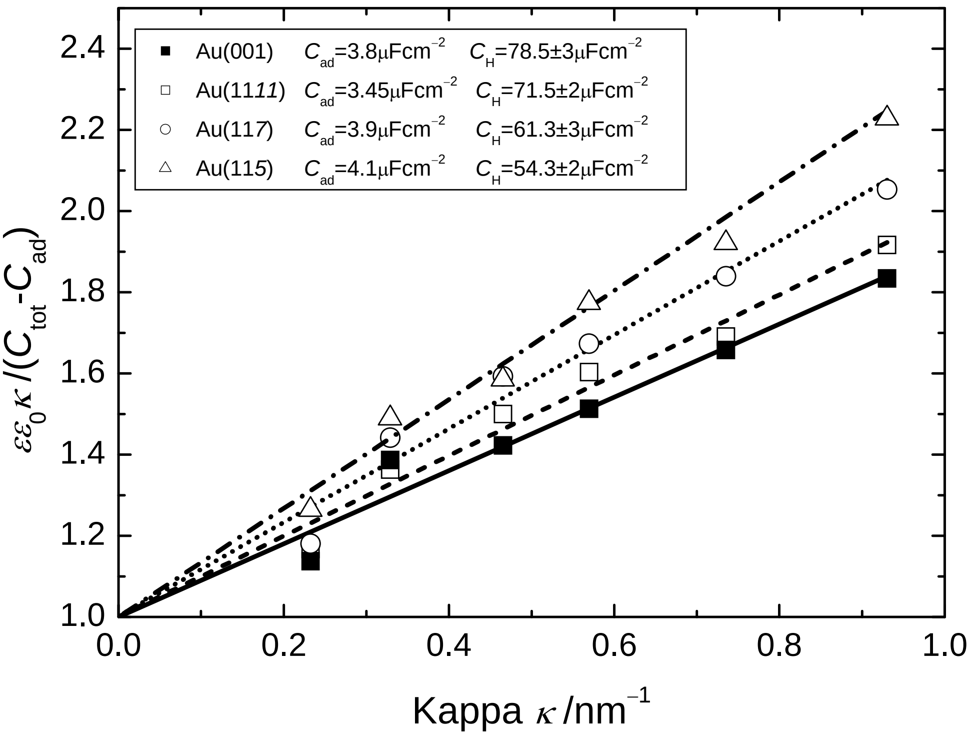
Au(001) C_{ad}=3.8μFcm^{-2} C_H=78.5±3μFcm^{-2}
Au(11*11*) C_{ad}=3.45μFcm^{-2} C_H=71.5±2μFcm^{-2}
Au(11*7*) C_{ad}=3.9μFcm^{-2} C_H=61.3±3μFcm^{-2}
Au(11*5*) C_{ad}=4.1μFcm^{-2} C_H=54.3±2μFcm^{-2}
$\varepsilon\varepsilon_0\kappa/(C_{tot}-C_{ad})$
Kappa κ /nm^{-1}
1.0
1.2
1.4
1.6
1.8
2.0
2.2
2.4
0.0
0.2
0.4
0.6
0.8
1.0

Fig. 3

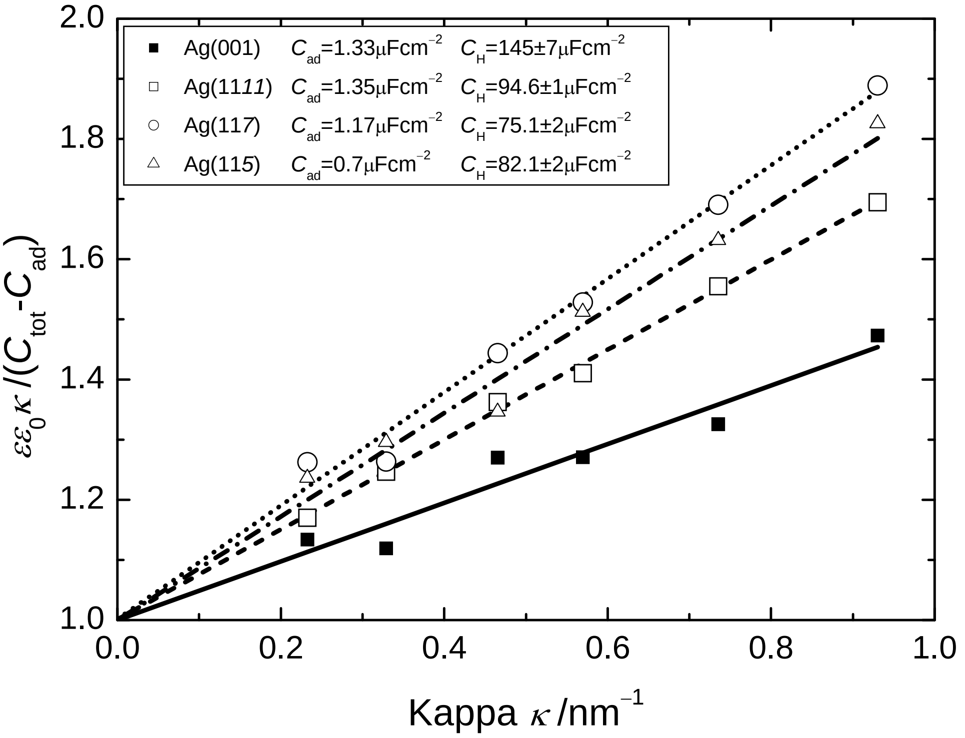
Ag(001) C_{ad}=1.33μFcm^{-2} C_H=145±7μFcm^{-2}
Ag(11*11*) C_{ad}=1.35μFcm^{-2} C_H=94.6±1μFcm^{-2}
Ag(11*7*) C_{ad}=1.17μFcm^{-2} C_H=75.1±2μFcm^{-2}
Ag(11*5*) C_{ad}=0.7μFcm^{-2} C_H=82.1±2μFcm^{-2}
$\varepsilon\varepsilon_0\kappa/(C_{tot}-C_{ad})$
Kappa κ /nm^{-1}
1.0
1.2
1.4
1.6
1.8
2.0
0.0
0.2
0.4
0.6
0.8
1.0

Fig. 4

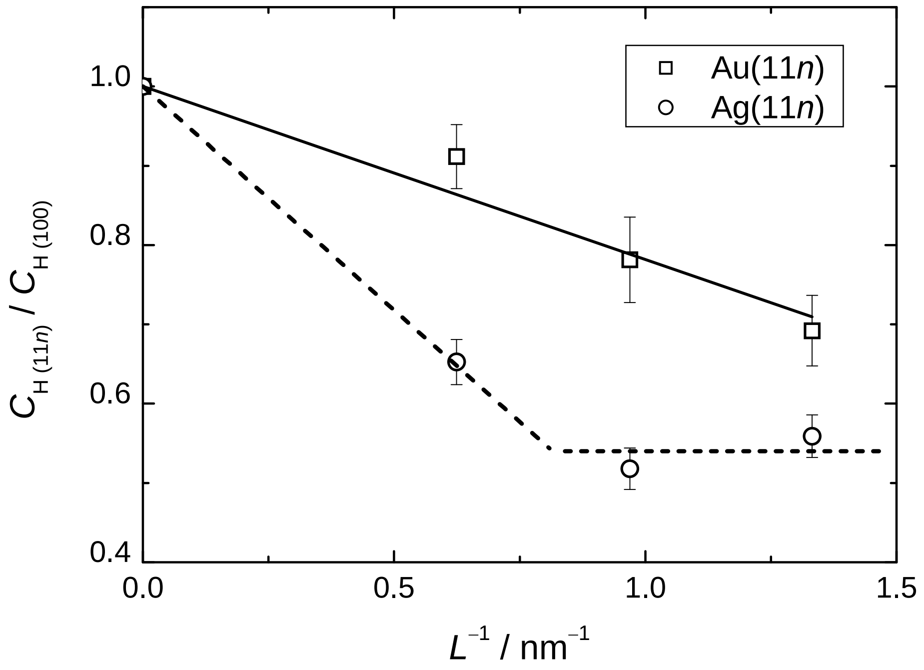
Au(11*n*)
Ag(11*n*)
$C_{H\,(11n)}\,/\,C_{H\,(100)}$
1.0
0.8
0.6
0.4
0.0
0.5
1.0
1.5
L^{-1} / nm^{-1}

Fig. 5

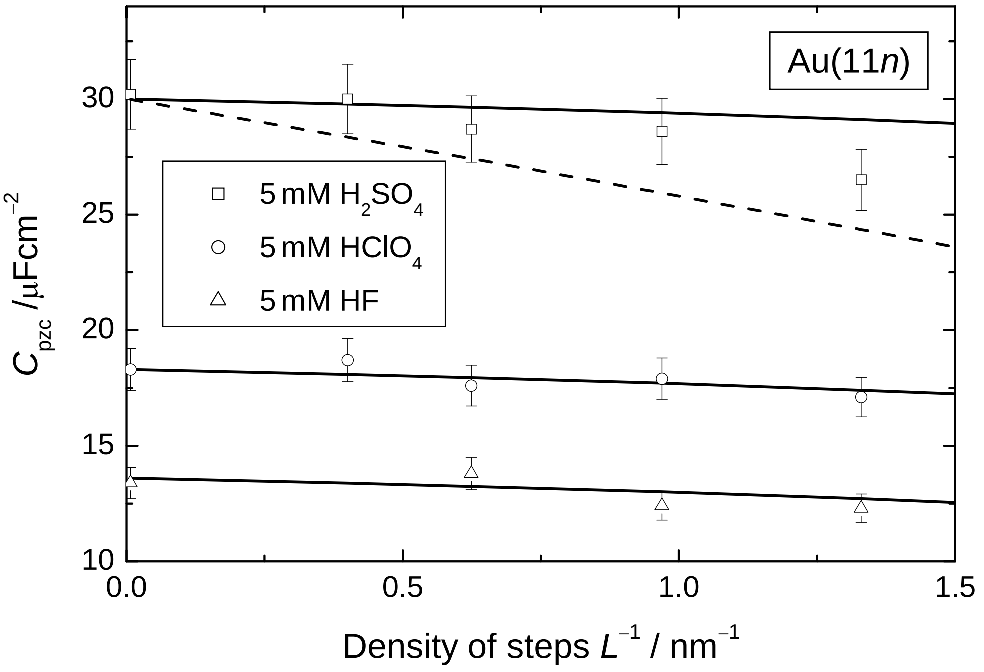
Au(11*n*)
5 mM H_2SO_4
5 mM $HClO_4$
5 mM HF
C_{pzc} /μFcm^{-2}
30
25
20
15
10
0.0
0.5
1.0
1.5
Density of steps L^{-1} / nm^{-1}

Fig. 6

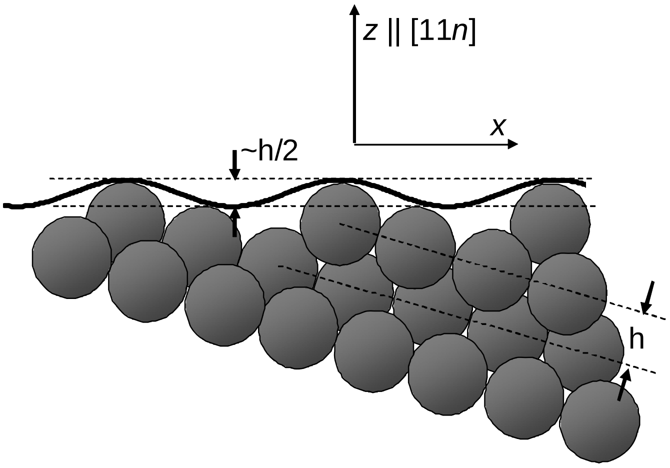

Fig. 7

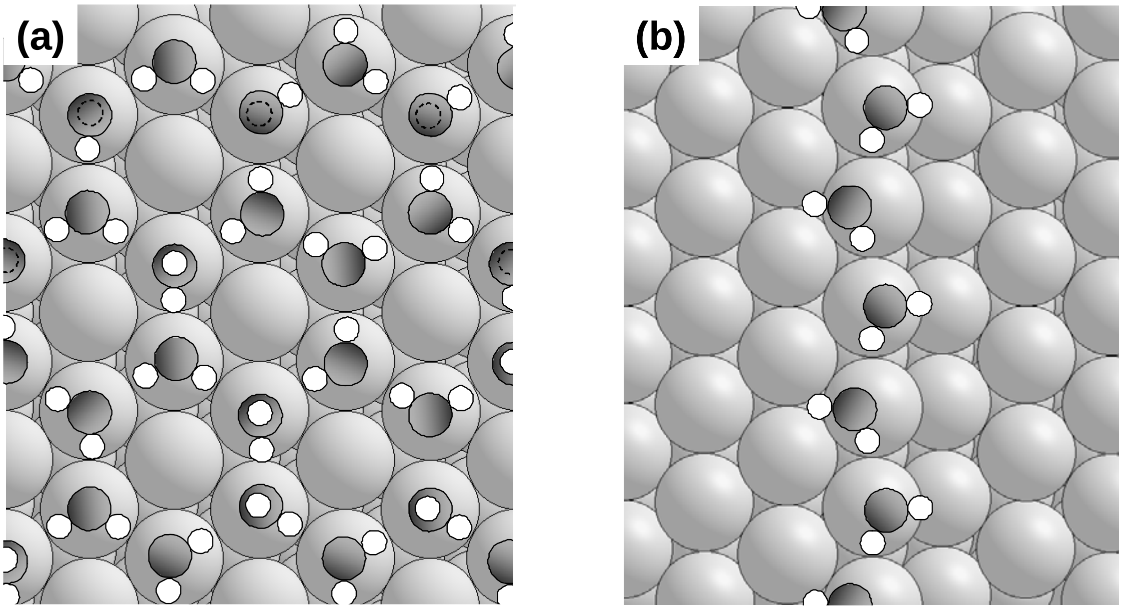

Fig. 8